

ORIGINAL RESEARCH PAPER
Pages:258-270

Planar Multibeam Array Antenna with Rotman Lens Beamformer for 5 GHz Band Wireless Applications

Farid Shokouhi and Zaker Hossein Firouzeh

Department of Electrical and Computer Engineering, Isfahan University of Technology,
Isfahan 8415683111, Iran

farid.shokouhi84@gmail.com, zhfirouzeh@cc.iut.ac.ir

corresponding author: zhfirouzeh@cc.iut.ac.ir

DOI: 10.22070/jce.2021.14278.1184

Abstract- A planar multi-beam array with a co-planar Rotman lens beamformer is introduced for wireless applications. The array consists of 8 linear series-fed subarrays with proximity-coupled patch elements. The Rotman lens feeds the subarrays through coupling slots. To reduce beam squinting, the subarrays are fed from the center. The coupling slot feeds each arm of a subarray 180° out of phase. To compensate out-of phase feeding, two feeding arms of each subarray are designed in the opposite direction. Also, cross-polar radiation is reduced significantly. In order to reduce the size of radiating patches to fit within array cell size, they are formed by four sub-patches with indentions and are fed by microstrip line from feed layer with two matching sections to improve the bandwidth. Measured results of the array structure in terms of the S-parameter of beam ports and radiation patterns are presented.

Index Terms- beamforming network, microstrip antenna, planar array, rotman lens, series-feds.

I. INTRODUCTION

Modern wireless communication relies on high gain directional antenna and beamforming networks. With the growing demand for high-capacity point-to-point and point to multipoint communication links, and the development of 5G networks, multi-beam antennas have attracted lots of attention [1]. Beamformers are essential for any multi-beam antenna system for the electronic generation of multiple beams from the same aperture. In phased array systems, antenna beam steering is implemented by use of phase shifters and attenuators in 1D and 2D arrays. The cost of such arrays could be very high because of the high number of discrete RF components needed to implement for beam steering, and the fabrication process is also a challenging task. So, the application is mainly limited to radar and satellite communications. On the other side, when several simultaneous multiple

beams are needed, passive beamforming networks like Butler matrix and Rotman lens are low cost and easy to fabricate candidates for beamformer design of antenna systems [2]. Such passive beamformers are good candidates for tracking and radar applications as switched beam antennas, as well as multiple simultaneous beam communication networks [3, 4]. The passive beamformers can be generally divided into two categories; circuit-based beamformers like Butler and Blass matrix and lens-based beamformers like Rotman and Ruze lenses. Lens-type beamformers have advantages of wider bandwidth and simple implementation rather than circuit-based beamformers [3]. Planar microstrip antennas have been used for different communication and radar applications due to their low cost, lightweight, and compact size [4, 5]. Different architectures are proposed for the implementation of microstrip antenna arrays [6]. Since the fabrication process of microstrip planar antenna arrays is the same as planar beamforming networks, the planar arrays are appropriate to use with planar beamforming networks. So, the antenna array and beamformer can be effectively integrated into the same board. As a result, this reduces implementation cost and also saves required space for the antenna system. Furthermore, it improves the system performance because of the elimination of intermediate connections and circuits. The Rotman lens generally consists of three sections. Beam ports that are input ports of the beamformer are related to different beam angles—array ports and connecting lines that connect lens surface to the antenna elements. The lens section provides proper collimation of RF power to each beam port to direct the antenna beam to the desired angle. The lens section could also be merged with dummy ports to eliminate spillover of RF power.

Rotman lens is used for linear 1D scanning and 2D scanning arrays [7-9]. 2D scanning with Rotman lens needs 3D lens design [10] or stacking up 2D lenses [7]. For linear scanning applications, fan-beam arrays that beam widths are only considered in one dimension are designed [11]. Multi-layer design configurations are presented in [12-14] for millimeter-wave radar design. In [12], a multi-layer structure is introduced with Rotman lens for beamforming and substrate integrated waveguide slotted array for X-band application. In [13], the Rotman lens is used to feed linear series-fed array and integrate with TX/RX modules. In both designs, power is delivered to radiating array via aperture coupling, and phase matching is done by introducing offsets in coupling slot positions. In [14], the C-band Rotman lens array is designed by slot coupling and circularly polarized elements. For all three preceding designs, the array is fed from one side of the antenna array. This feed mechanism saves more space for a large Rotman lens however, it limits the bandwidth due to beam squint of array pattern. Offsetting the slots in [12, 13] simplifies the design of the Rotman transmission line section and improves insertion loss of the lens.

In this paper, a new center-fed design for high gain and low-profile planar multi-beam antenna based on Rotman lens beamformer and series-fed planar microstrip array is introduced for Wi-Fi applications. To have 1D beam scanning capability, a series-feeding technique is used. A new

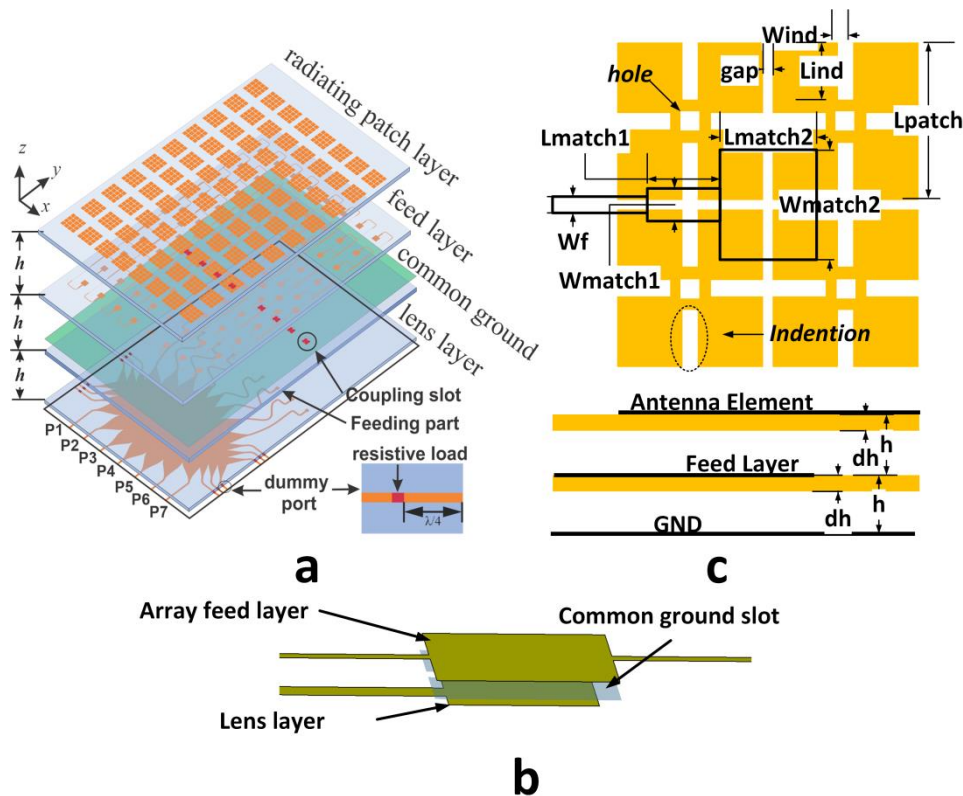


Fig. 1 a) Antenna structure with multiple layers. b) coupling between rotman lens layer and array feed layer. c) Radiating patch structure. Parameters of the patch antenna are $L_{patch}=7\text{mm}$, $gap=0.75\text{mm}$, $Wind=4\text{mm}$, $Lind=1\text{mm}$, $W_{match1}=3.2\text{mm}$, $L_{match1}=9.36\text{mm}$, $W_{match2}=9.28\text{mm}$, $L_{match2}=9.28\text{mm}$, $Wf=1\text{mm}$, $h=1\text{mm}$, $dh=0.25\text{mm}$.

approach for coupling between Rotman lens and microstrip array is presented based on vertical coupling. The structure of the planar coupling between the Rotman lens and the microstrip array with series feeding provides a compact and wideband feeding antenna array resulting in low profile integration of beamforming and radiating array. The compact series feeding also reduces dissipation loss and improves overall efficiency. Proximity-coupled microstrip patch antenna elements are also miniaturized to fit in the array unit cell area. The whole structure was built using FR4 epoxy laminate to reduce the overall cost of implementation, and spacing was placed between layers to compensate for the high losses of FR4 laminate.

The remainder of the paper is as follows; the array antenna configuration is presented in section 2. This section presents the array element structure and array feed design in Sections 3 and 4, respectively. Rotman beamforming network is designed in Section 5. Simulation results are discussed in Section 6. Finally, the fabrication and measurement results are reported in Section 7. Concluding remarks are explained in the last section.

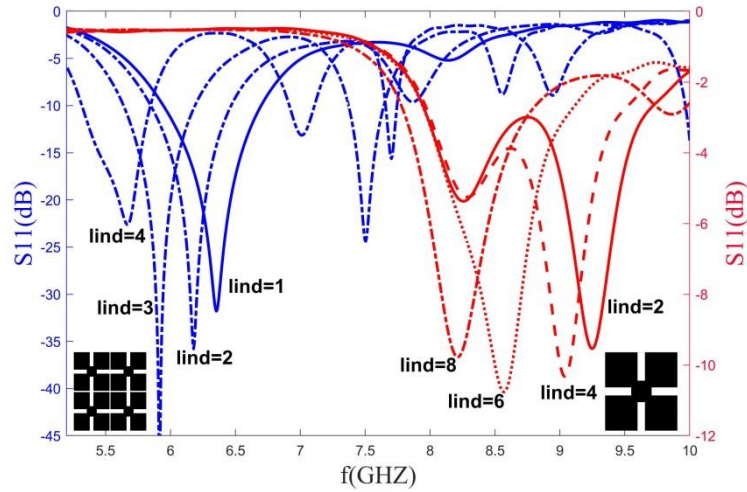


Fig. 2 S-parameters of radiating patch with various indentation sizes and the number of sub-patches.

II. ARRAY ANTENNA CONFIGURATION

Fig. 1-a shows the structure of the array antenna based on the Rotman beamforming network. The array is implemented using four low-cost FR4 epoxy layers with 0.25mm thickness and with $\epsilon_r=4.4$ and $\tan\delta=0.02$. Spacing is added between the layers to compensate for high dielectric losses of FR4 dielectric material. The array consists of 8 lines of 10×1 series-fed proximity coupling patch antennas fed from the Rotman lens array ports on the other side of the common ground plane through wideband slot-coupled transitions. The Rotman lens is connected to the array via 8×1 linear array form. Although feeding on the center of the series-fed line extends array size from one side of the array, it prevents the beam squint due to frequency changes [15, 16], and as a result, it widens the bandwidth of the feed network. Feeding on the array center also causes the Rotman beam ports to lower array sides which is suitable for integration with RF circuitry. Each series-fed line consists of two subarrays. Each arm of the subarray consists of 1×5 proximity coupled patch antenna with 20dB-Taylor taper distribution. T-junctions in the traveling wave linear array configuration are designed with quarter-wave transformers along the feed-line to achieve the desired taper.

III. ARRAY ELEMENT DESIGN

The proximity-coupled microstrip patch antenna is used as radiating element of the array. The antenna structure is shown in Fig. 1-b. Since the limitations of the array unit cell resulting from frequency and scanning parameters, antenna patch size should be small enough to fit in the unit cell area and also not cover the array feed-line section to avoid grating lobe. To reduce the resonance frequency of the patch antenna, it is divided into four sub-patches with close spacing, as shown in Fig. 1-b. This technique is widely known and used in fractal antenna design for miniaturization and

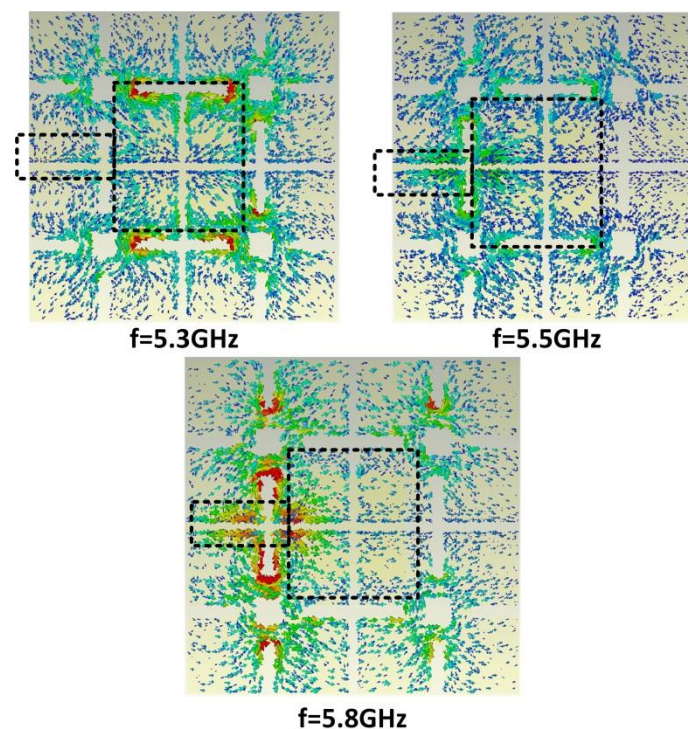


Fig. 3. E-field distribution of patch for different frequencies

bandwidth enhancement of antennas [17]. To further reducing of working frequency four indentions and central holes are also added to sub-patches.

The addition of sub-patches with indentions makes current lines longer around the patches. The antenna feed line consists of two matching sections over the ground plane. Feeding structure and radiating patches are etched on FR4 substrate with a thickness of 0.25 mm and 0.75 mm spacing between ground, feed network, and the radiating layers. The spacing between layers reduces dielectric loss to improve antenna efficiency. Geometry parameters of the patch antenna are tuned to radiate at 5.5GHz center frequency with maximum bandwidth. Parameters of the patch antenna are $L_{patch} = 7\text{mm}$, $gap = 0.75\text{ mm}$, $W_{ind} = 4\text{ mm}$, $L_{ind} = 1\text{ mm}$, $W_{match1} = 3.2\text{ mm}$, $L_{match1} = 9.36\text{ mm}$, $W_{match2} = 9.28\text{ mm}$, $L_{match2} = 9.28\text{ mm}$, $W_f = 1\text{ mm}$, $h = 1\text{ mm}$, $dh = 0.25\text{ mm}$. S_{11} of the antenna element for a single patch and four tightly spaced sub-patches is shown in Fig. 2 with feed parameters. Note that the overall patch dimension is the same for the two configurations. As it can be seen, using a sub-patch design reduces the resonance frequency of the antenna from 8.5 GHz to 5.5 GHz. An increase the length of indentation further reduces resonance frequency. For sub-patch design, 540 MHz bandwidth for 10dB return loss (RL) is achieved over the frequency range of 5.34GHz to 5.88 GHz. E-Field distribution for three different frequencies is also shown in Fig. 3. As it can be observed, field lines are denser around sub-patch indentions. Indention elongates field lines leading to lower working frequency. On the other side, E-Field for 5.3GHz is stronger around horizontal indentions

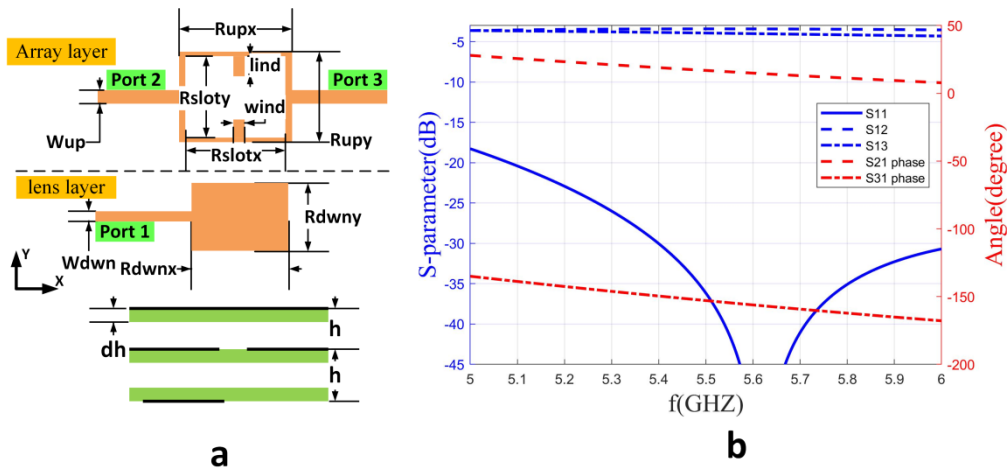


Fig. 4 a) Structure of vertical transition. b) Simulated results of s-parameter and phase of vertical transition. Parameters (in mm) are Rdwnx=3.4, Rdwny=3, Rupx=5.7, Rupy=5.1, Rslotx=5.9, Rsloty=5.2, lind=2.3, wind=1.3, Wup=1, Wdwn=3.5, h=1mm, dh=0.25.

that are around wider feed section corresponding to lower frequency matching, while E-Field in 5.7 GHz is focused around smaller feed section that improves matching in higher frequencies.

IV. ARRAY FEED DESIGN

The feed section consists of two 1×5 series T-junction power dividers in traveling waveform. Each arm of two 1×5 arrays is fed by an aperture coupled power divider. The symmetric power divider feeds two array arms with the 180 deg phase difference. To feed array elements in phase, the feed arm of T-junctions is mirrored in each side of the sub-array. On the other side of the antenna, element feed arms are also mirrored along the symmetry line of the Rotman lens. With this configuration, cross-polar field elements in both sides of the center feed and both sides of the symmetry line of the Rotman lens cancel out each other.

A. Feed Network

To feed linear sub-array of proximity-coupled patch elements, series of T-junctions are cascaded. For the equal phased feeding of elements, the junction spacing is set to one guided wavelength. To obtain desired array taper and good matching between T-junctions, transmission lines with a length of $\lambda_g/4$ and $3\lambda_g/4$ length where $\lambda_g = 46\text{mm}$ for the center frequency of 5.5 GHz. Line widths are calculated according to the desired taper. Detailed design considerations for series-fed patch antennas have been discussed in [5]. Some modifications are made in patch feed parameters to compensate for the array feed network and mutual coupling effects of patch elements.

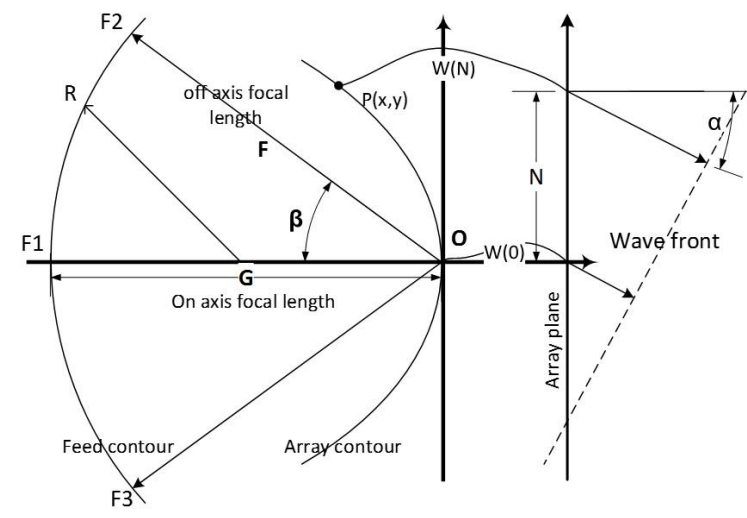


Fig. 5 Geometry of Rotman lens with parameters.

B. Vertical Coupling

To couple the Rotman beamformer to the feed network layer, a vertical coupling is used. Authors have reported several designs for vertical coupling between layers [17-20]. Wideband aperture-coupled transitions are designed by different authors [17, 19]. In this work, to have compact and easy to fabricate transition, rectangular slot patches are used. Because the feed layer divides power between two array arms, the transition also acts as an equal power divider.

The structure of the slot coupling is shown in Fig. 4-a. To minimize spurious radiation from the rectangular part of the slot in the feed layer and also to prevent it from interfering with patch elements, its size should be as small as possible. This limitation restricts the bandwidth of the slot. Therefore, optimization is necessary to obtain the widest bandwidth while the rectangular patch size is kept small. Two indents are also added to the coupling slots to have an additional parameter for optimization to improve the slot bandwidth. Because the effective permittivity of two dielectric layers is low, the layer thickness should be small enough to have sufficient coupling through the aperture. On the other hand, the higher thickness of the feed layer may excite powerful surface waves that degrade radiation performance. This limitation for the layer thickness limits the spacing between the feed layer and patch antenna. The detailed design procedure of the coupling slot is presented in [17]. Parameters for vertically coupling slot as shown in Fig. 5 are $R_{dwnx}=3.4\text{mm}$, $R_{dwny}=3\text{mm}$, $R_{upx}=5.7\text{mm}$, $R_{upy}=5.1\text{mm}$, $R_{slotx}=5.9\text{mm}$, $R_{sloty}=5.2\text{mm}$, $l_{ind}=2.3\text{mm}$, $w_{ind}=1.3\text{mm}$, $W_{up}=1\text{mm}$, $W_{dwn}=3.5\text{mm}$, $h_1=h_2=1\text{mm}$, $dh_1=0.25\text{mm}$. S-parameter of the coupling slot is shown in Fig. 4-b 900 MHz bandwidth for 20dB return loss from 5.1GHz to 6GHz is achieved. The magnitude difference between the two output ports is less than 0.8 dB from 5.2 to 6 GHz. The phase difference between the two outputs is changes from 164° at 5GHz to 174° at 6GHz.

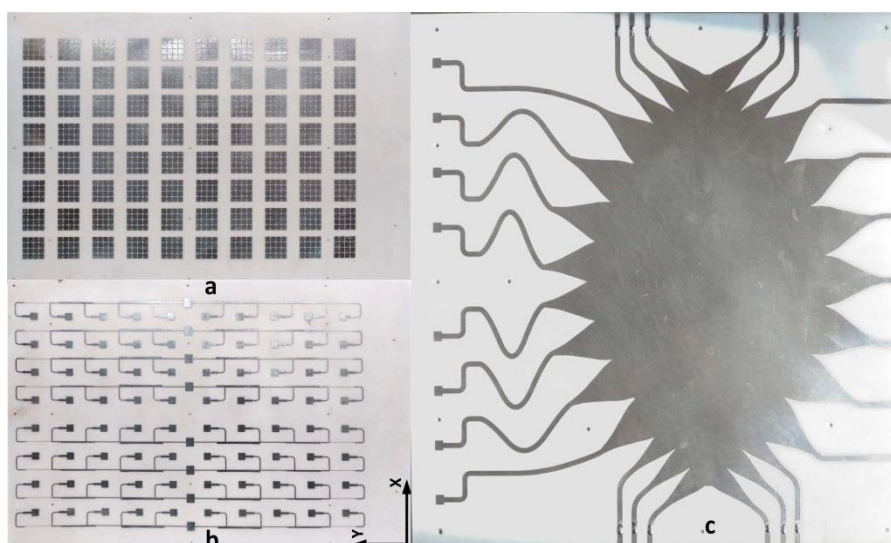


Fig. 6. Fabricated layers of array antenna structure. a) Radiating patch layer. b) Feeding layer. c) Rotman lens layer.

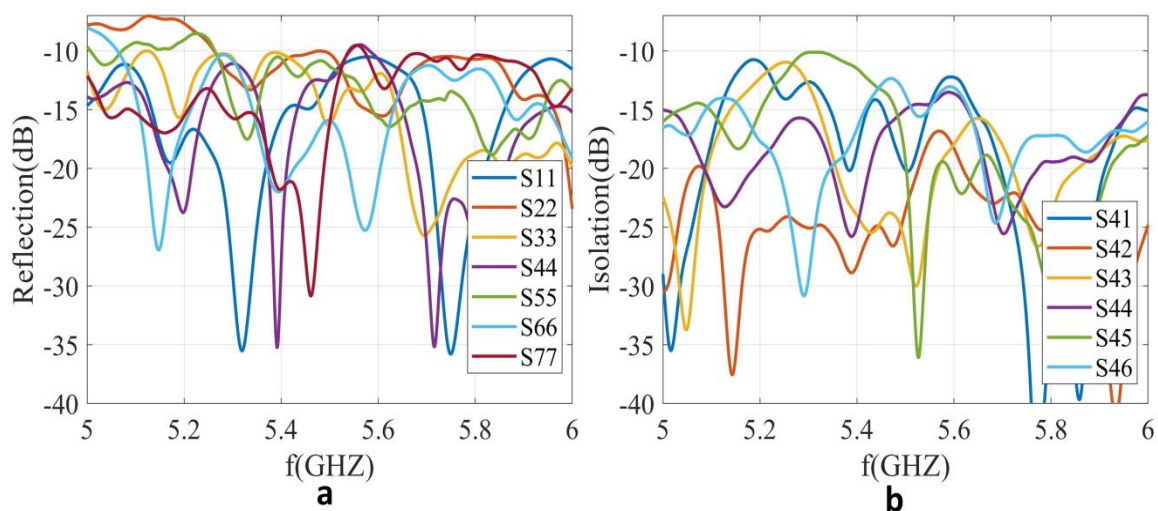


Fig. 7. a) Measured reflection from various beam ports. b) Measured mutual coupling between port No.4 and other ports.

V. ROTMAN BEAMFORMING DESIGN

Rotman beamformer structure is presented in Fig. 5. In the Rotman lens design, three ideal focal points correspond to broadside, and two outermost scan angles form feed contour. In [21], the outermost beam port angles are the same as maximum scan and not necessarily equal to array port height. However, based on the guidelines in [22] for the maximum power delivery to the array ports, both the beam and array contour height should be the same.

Table I. Parameter definitions of rotman lens and their values

Definition	Value
Maximum position of radiating elements(m)	0.137
Maximum scanning angle	30
Focal angle	38
Array spacing(m)	0.35
Num. of beam ports	7
Num. of Array ports	8

In [1, 2], the modified design equations with an extra parameter for the feed contour height have been presented. The rotman lens is designed based on design equations presented in [1, 2], and main design parameters are summarized in

Table I.

Beam and array ports are tapered to the lens point to match the microstrip line to the radial waveguide of the lens section. The taper design procedure has been explained in [23]. Based on the guidelines in [24] for sidewall design, 12 dummy ports are formed for maximum absorption of lens spillover. The dummy ports are terminated with a 50 ohm SMD resistor with $\lambda_g/4$ spacing from the edge of the substrate.

The fabricated beamformer is shown in Fig. 6-c. The beamformer consists of 7 beam ports for scan angles of $\pm 30^\circ$, $\pm 20^\circ$, $\pm 10^\circ$, 0° fed by eight array ports. Based on (3), to avoid grating lobes, the element spacing for a maximum of $\pm 30^\circ$ scan angle at a frequency of 5.8GHz is 34mm.

VI. RESULTS AND DISCUSSION

The entire array and beamformer prototype are fabricated, and its layers are shown in Fig. 6. The array feed layer and patch layer are shown in Fig. 6-b and Fig. 6-a, respectively. Rotman lens structure is shown in Fig. 6-c. The total antenna dimensions are 568mm \times 350mm.

For structure rigidity and suppression of back radiation from the coupling slots, an aluminum reflector plane is used as the backplane with 15mm spacing from the Rotman lens layer. The reflection and mutual coupling between beam ports are shown in Fig. 7-a and Fig. 7-b, respectively. Bandwidth for -10 dB reflection is over 5.25GHz to 6GHz, and mutual coupling between center port (port 4) and other ports are lower than 15dB over a range of 5.65-6GHz and lower than 10dB for 5-6GHz. The main bandwidth limiting parameters of design is the narrow bandwidth of the array element and the limited bandwidth of the series feed.

Measured E-plane (xz) radiation patterns at 5.7GHz are shown in Fig. 8. The HPBW's are approximately 11° , 9° , 11° , 10° , 10° , 8° for ports 1 to 7, and the related beam directions are -30° ,

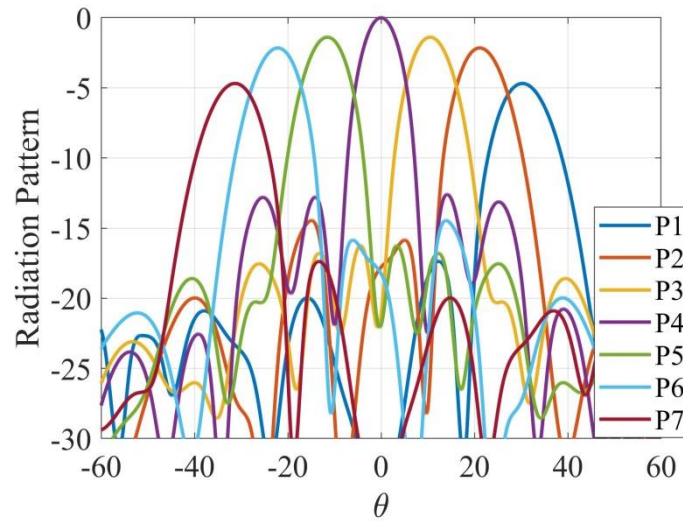


Fig. 8 Measured radiation patterns for excitation from various beam ports.

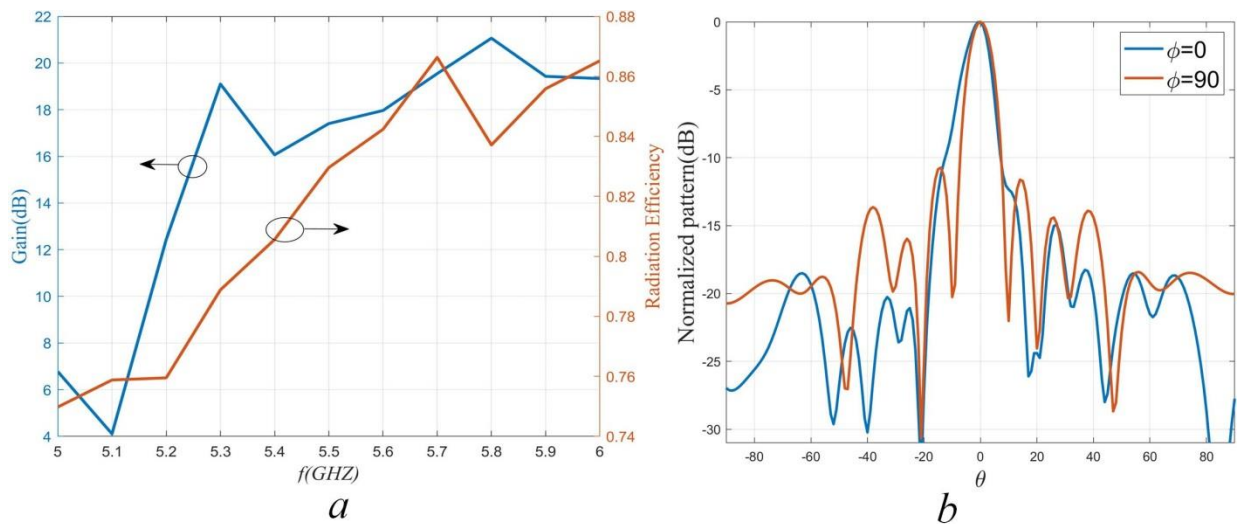


Fig. 9. a) Simulated gain and radiation efficiency of the array. b) Normalized antenna array pattern in $\phi=0$ and $\phi=90$ planes at 5.5GHz.

-21° , -10° , 0° , $+11^\circ$, $+19^\circ$, 31° , respectively. Slight variations from designed angles are because of fabrication and measurement tolerances. Crossover between adjacent ports is -3dB for $\pm 30^\circ$ angular section.

The simulated gain and radiation efficiency of the proposed antenna are presented in Fig. 9a. As we can see, the gain is higher than 16dB for frequencies above 5.25 GHz and is 21 dB in 5.8 GHz . The radiation efficiency is also higher than 76 percent for frequencies above 5.25 GHz .

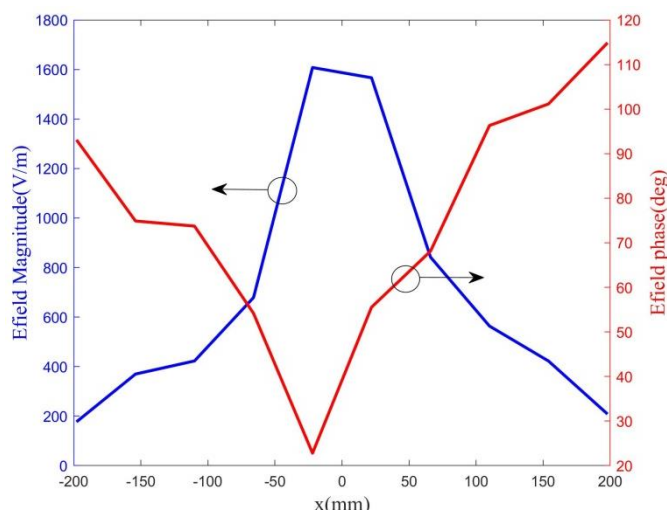


Fig. 10. E-field magnitude and phase distribution of central array elements along the x-direction at 5.5 GHz

Antenna array gain in $\varphi=0$ and $\varphi=90$ at 5.5GHz is also presented in Fig. 9b. It is observed that in the $\varphi=0$ plane with amplitude taper is applied to the array feed network, we have 15dB sidelobe level. Despite a sidelobe in 27 degrees off the broadside, there is no other sidelobe above 18dB in $-90<\theta<90$ region. However, the sidelobe level in the $\varphi=90$ plane in which array steering is applied can be as high as 14dB. The magnitude and phase of the E-field distribution of the proposed design over the center array elements along the x dimension at 5.5 GHz are shown in Fig. 10. The field has an amplitude taper along the x-dimension of the array.

VII. CONCLUSION

In this paper planar multi-beam array with a Rotman lens beamformer is designed and fabricated. The multi-layer structure of the array and beamformer is compact and highly integrated, and suitable for various wireless applications like point to multipoint networks. Slot coupling of the Rotman lens layer to the array layer and proximity coupling of radiating patches eliminating the need for vias which complicate the design and fabrication. Linear series-fed subarray design reduces feed-line losses and, at the same time, provides a compact structure to feed radiating patches.

The side lobe of the array pattern in elevation direction could also be controlled with proper design of series feed-line. The feeding mechanism and the direction of feed lines eliminate cross-polar field elements and improve the sidelobes. Radiating patches are also miniaturized in order to fit in the array unit cell and to prevent from interfering with the feed network. The Fabricated structure presents acceptable results in 5-6 GHz frequency rang in terms of reflection and isolation between beam ports. The measured patterns also verify Rotman lens design parameters and array configuration.

VIII. ACKNOWLEDGMENTS

The authors would like to thank the Research Institute for Avionics, Isfahan University of Technology, Iran, for supporting this project.

REFERENCES

- [1] T. Katagi, S. Mano, and S. Sato, "An improved design method of Rotman lens antennas," *IEEE Trans. Antennas Propag.*, vol. 32, no. 5, pp. 524-527, May 1984.
- [2] P. K. Singhal, P. C. Sharma, and R. D. Gupta, "Rotman lens with equal height of array and feed contours," *IEEE Trans. Antennas Propag.*, vol. 51, no. 8, pp. 2048-2056, Aug. 2003.
- [3] P. S. Hall and S. J. Vetterlein, "Review of radio frequency beamforming techniques for scanned and multiple beam antennas," *IEE Proceedings H (Microwaves, Antennas and Propag.)*, vol. 137, no. 5, pp. 293-303, Oct. 1990.
- [4] R. Bayderkhani and H. R. Hassani, "Wideband and Low Sidelobe Slot Antenna Fed by Series-Fed Printed Array," *IEEE Trans. Antennas Propagation*, vol. 58, no. 12, pp. 3898-3904, Dec. 2010.
- [5] F. Y. Kuo and R. B. Hwang, "High-Isolation X-Band Marine Radar Antenna Design," *IEEE Trans. Antennas Propagation*, vol. 62, no. 5, pp. 2331-2337, May 2014.
- [6] D. M. Pozar, D. H. Schaubert, I. Antennas, and P. Society, *Microstrip Antennas: The Analysis and Design of Microstrip Antennas and Arrays*. Wiley-USA, 1995.
- [7] K. K. Chan and S. K. Rao, "Design of a Rotman lens feed network to generate a hexagonal lattice of multiple beams," *IEEE Trans. Antennas Propagation*, vol. 50, no. 8, pp. 1099-1108, Aug. 2002.
- [8] H.-I. Lin and W.-J. Liao, "A beam switching array based on Rotman lens for MIMO technology," in *Microwave and Millimeter Wave Technology (ICMMT), 2012 International Conference on*, 2012, vol. 2, pp. 1-4.
- [9] D. Nussler, R. Brauns, and H.-H. Fuchs, "A two dimensional lens stack design for 94 GHz," in *2009 German Microwave Conference*, pp. 1-4.
- [10] G. Sole and M. Smith, "Multiple beam forming for planar antenna arrays using a three-dimensional Rotman lens," *IEE Proceedings H (Microwaves, Antennas and Propag.)*, vol. 134, no. 4, pp. 375-385, Aug. 1987.
- [11] Y. Tao and G. Delisle, "Lens-fed multiple beam array for millimeter wave indoor communications," in *IEEE Antennas and Propagation Society International Symposium*, 1997. Digest, vol. 4, pp. 2206-2209.
- [12] Y. Liu, H. Yang, D. Huang, and J. Zhu, "A low sidelobe multi-beam slot array antenna fed by rotman lens," in *Antennas & Propagation Conference (LAPC), 2016 Loughborough*, 2016, pp. 1-5.
- [13] W. Lee, K. Young Sub, J. Kim, and Y. J. Yoon, "Multi-layer beamforming lens antenna array with a new line design for millimeter-wave system-in-package applications," in *Proceedings of the 5th European Conference on Antennas and Propagation (EUCAP)*, 2011, pp. 2954-2958.
- [14] S. Peik and J. Heinstadt, "Multiple beam microstrip array fed by Rotman lens," in *Antennas and Propagation, 1995., Ninth International Conference on (Conf. Publ. No. 407)*, 1995, vol. 1, pp. 348-351.
- [15] S. Park, Y. Tsunemitsu, J. Hirokawa, and M. Ando, "Center feed single layer slotted waveguide array," *IEEE Trans. Antennas Propagation*, vol. 54, no. 5, pp. 1474-1480, May 2006.
- [16] A. Bisognin et al., "A new symmetric feeding technique for a broadband series-fed antenna-array," in *Antennas and Propagation Society International Symposium (APSURSI)*, 2013 IEEE, 2013, pp. 2183-2184.
- [17] Z. Tao, J. Zhu, T. Zuo, L. Pan, and Y. Yu, "Broadband microstrip-to-microstrip vertical transition design," *IEEE Microwave and Wireless Components Letters*, vol. 26, no. 9, pp. 660-662, Sept. 2016.

- [18] S. A. Wartenberg and Q. H. Liu, "A coaxial-to-microstrip transition for multi-layer substrates," *IEEE Trans. Microw. Theory Tech.*, vol. 52, no. 2, pp. 584-588, Feb. 2004.
- [19] A. Abbosh, "Ultra wideband vertical microstrip–microstrip transition," *IET Microwaves, Antennas & Propagation*, vol. 1, no. 5, pp. 968-972, 2007.
- [20] F. P. Casares-Miranda, C. Viereck, C. Camacho-Peñalosa, and C. Caloz, "Vertical microstrip transition for multi-layer microwave circuits with decoupled passive and active layers," *IEEE Microwave and Wireless Components Letters*, vol. 16, no. 7, pp. 401-403, July 2006.
- [21] W. Rotman and R. Turner, "Wide-angle microwave lens for line source applications," *IEEE Trans. Antennas Propag.*, vol. 11, no. 6, pp. 623-632, Nov. 1963.
- [22] P. K. Singhal, R. D. Gupta, and P. C. Sharma, "Recent trends in design and analysis of Rotman-type lens for multiple beamforming," *International Journal of RF and Microwave Computer-Aided Engineering*, vol. 8, no. 4, pp. 321-338, 1998.
- [23] J. Dong and A. I. Zaghoul, "Hybrid Ray Tracing Method for Microwave Lens Simulation," *IEEE Trans. Antennas Propag.*, vol. 59, no. 10, pp. 3786-3796, Oct. 2011.
- [24] E. O. Rausch and A. F. Peterson, "Rotman lens design issues," in *Antennas and Propagation Society International Symposium, 2005 IEEE*, vol. 2, pp. 35-38.